CHAPTER IV
RESULTS AND DISCUSSION

4.1 Catalyst Characterization

In this study, the HZSM-5 catalysts (SiO_2/Al_2O_3 = 195) synthesized obtained at crystallization temperature 150 °C for 24 h, 48 h, and 72 h are designated as HZ5A1, HZ5A2, and HZ5A3, respectively. The zeolites synthesized at crystallization temperature 180 °C for 24 h, 48 h, and 72 h are designated as HZ5B1, HZ5B2, and HZ5B3, respectively.

4.1.1 X-ray Diffraction

Figure 4.1 presents the XRD patterns of the reference and synthesized HZSM-5 zeolites. It shows the characteristic diffraction peaks corresponding to the pattern of commercial HZSM-5 zeolite. The high intensity peaks indicate that the catalysts have high crystallinity.

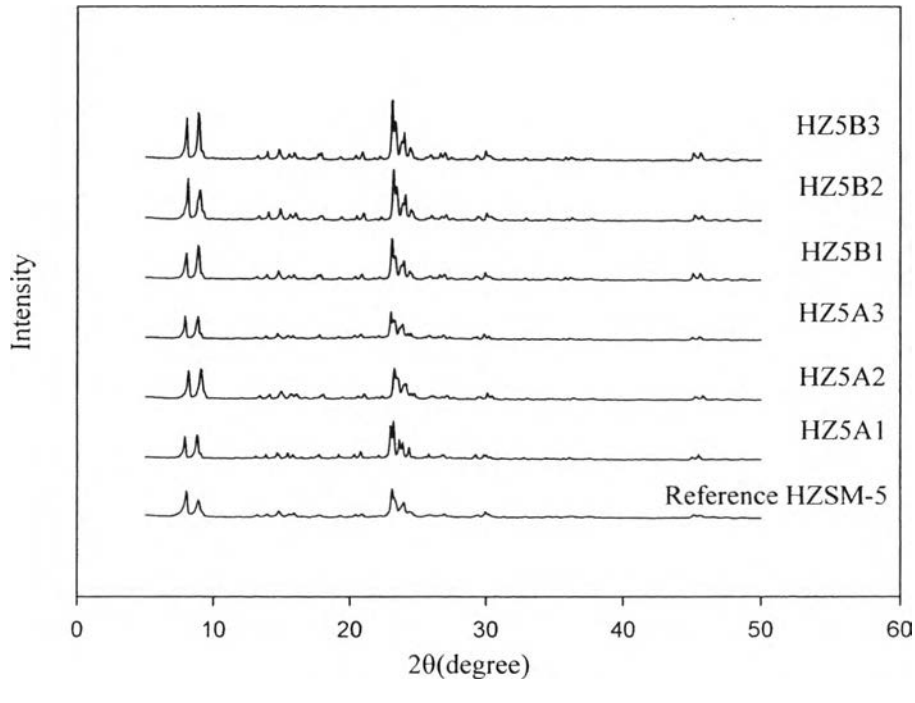

Figure 4.1 X-ray diffraction patterns of the synthesized HZSM-5 catalysts.

The peak intensity in the high diffractive angle (2θ = 23°) increased with increasing synthesized time and temperature. HZ5B3 showed the highest peak intensity peak because of long period of synthesized time and high synthesized temperature. As shown in Table 4.1, it was noticed that the synthesized HZSM-5 catalysts contained different crystallinity. The crystalllinity of HZSM-5 synthesized at 180 °C was higher than that of HZSM-5 synthesized at 150 °C. Besides, the crystalllinity of HZSM-5 synthesized for 72 h was higher than those of HZSM-5 synthesized for 48 h and 24 h, respectively.

Table 4.1 Relative crystallinity of catalysts

Catalyst	Relative crystallinity (%)
HZ5A1	48.45
HZ5A2	54.21
HZ5A3	57.24
HZ5B1	71.14
HZ5B2	85.58
HZ5B3	100.00

4.1.2 Catalyst Composition

The chemical composition of synthesized HZSM-5 catalysts was analyzed by X-ray fluorescence (XRF) technique. The results are summarized in Table 4.2. The Si/Al molar ratio was determined. HZ5A2 and HZ5B2 had Si/Al molar ratios of 88.5, and 90.9, respectively. It should be noticed that the crystallization temperature and aging time slightly affected (if used HZ5B2) to the catalyst composition. The theoretical acidity of catalysts determined based on the number of protons was attained according to its formula.

Table 4.2 The chemical compositions of synthesized HZSM-5 catalysts

Catalyst	Compound (wt %)			Si/Al[a] (molar ratio)	SiO_2/ Al_2O_3 (molar ratio)	Theoretical acidity (mmol/g)[b]
	Si	Al	Na			
HZ5A2	98.859	1.073	0.068	88.5	177	0.186
HZ5B2	98.842	1.063	0.095	89.3	179	0.181

[a]Chemical formula is $H_nAl_nSi_{96-n}O_{192}$
[b]Calculated values according to the information from International Zeolite Association (www.iza-online.org)

4.1.3 Surface Area Measurements

The surface characteristics of the synthesized catalysts determined by N_2 adsorption-desorption method are shown in Table 4.3. At 150 °C, the BET surface areas were significantly varied, ranging from 313 to 360 m^2/g, dependent on the crystallization time. However, the variation was insignificant (360-370 m^2/g) for those prepared at a higher temperature (180 °C). The variation of micropore volumes determined by NLDFT was more dependent on crystallization time at low temperature than at high temperature. Moreover, the total pore volume is considerably decreased with increasing temperature. Since, under hydrothermal synthesis, water, which is used to stabilize the porous products by filling the pores, vastly evaporates out of the pore at high temperature, as a result, the denser phases will become higher. Hence, the amount of porous structure will decrease (Ertl *et al*, 2008). The micropore-to-total pore volume (M/T) ratio was introduced as an indicator to be related to the catalyst activity. In addition, there was no change in pore diameter of the catalysts with different hydrothermal synthesis conditions.

Table 4.3 Surface characteristics of the synthesized HZSM-5 catalysts

Catalyst	BET Surface Area (m^2/g)	Micropore Volume [a](M) (cm^3/g)	Total Pore Volume[a] (T) (cm^3/g)	M/T Ratio	Pore Diameter [a] (Å)
HZ5A1	313.10	0.131	0.363	0.362	6.14
HZ5A2	332.40	0.146	0.386	0.378	6.14
HZ5A3	360.10	0.169	0.196	0.862	6.14
HZ5B1	367.00	0.174	0.176	0.989	6.14
HZ5B2	369.40	0.175	0.177	0.991	6.14
HZ5B3	361.30	0.171	0.173	0.986	6.14

[a] Determined by NLDFT method

4.1.4 Scanning Electron Microscopy (SEM)

Figure 4.2 shows SEM images of the synthesized HZSM-5 (HZ5A1, HZ5A2, HZ5A3, HZ5B1, HZ5B2, and HZ5B3). The crystal size of synthesized HZSM-5 is approximately 2-4 μm.

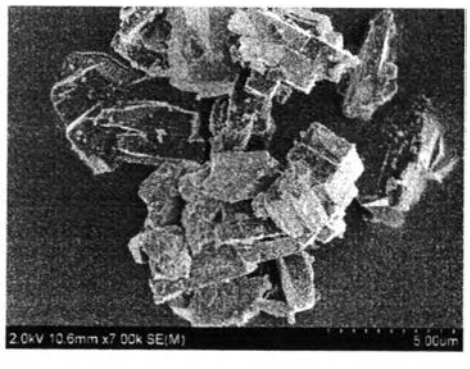

(HZ5A1)

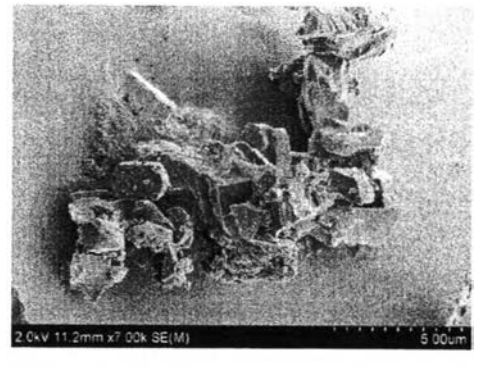

(HZ5B1)

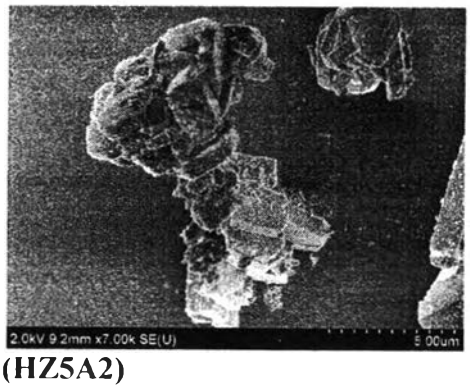

(HZ5A2)

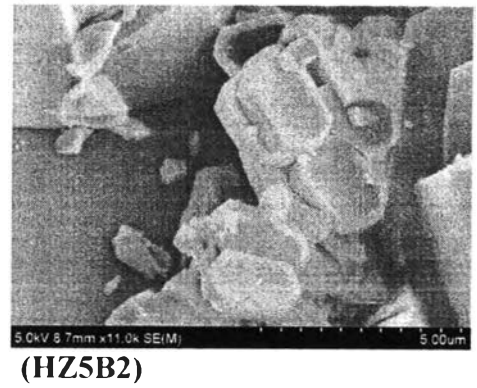

(HZ5B2)

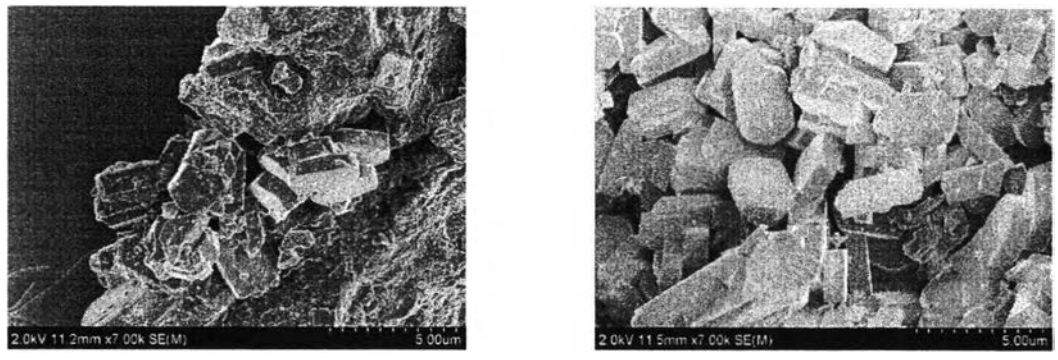

(HZ5A3) **(HZ5B3)**

Figure 4.2 SEM images of HZSM-5 (HZ5A1, HZ5A2, HZ5A3, HZ5B1, HZ5B2, and HZ5B3).

Table 4.4 Dimensions of HZSM-5 synthesized at different synthesis conditions

Catalysts	Crystallization temperature (°C)	Crystallization time (h)	Dimensions (microns)
HZ5A1	150	24	2.0 x 1.0 x 0.7
HZ5A2	150	48	2.5 x 1.5 x 0.5
HZ5A3	150	72	3.0 x 1.5 x 0.5
HZ5B1	180	24	2.0 x 1.5 x 0.5
HZ5B2	180	48	2.5 x 1.5 x 0.6
HZ5B3	180	72	3.5 x 2.0 x 0.7

Table 4.4 shows the dimensions of HZSM-5 synthesized at different conditions. The HZSM-5 synthesized at different conditions had different dimensions. The HZSM-5 synthesized at 180 °C was larger than that synthesized at 150 °C. Besides, a longer crystallization time resulted in a larger particle. The results are in good agreement with those reported by Kumar and co-workers (2002).

4.1.5 TG Analysis

Thermogravimetric analysis was used to determine thermal decomposition of the uncalcined ZSM-5 and uncalcined HZSM-5 (HZ5A3) catalysts in order to obtain the suitable calcination temperature. The results are shown in

Figure 4.3. The TG curve for uncalcined ZSM-5 shows two main weight loss regions. The first region, between 150 °C and 200 °C, is caused by the removal of water, whereas the second region, between 400 °C and 500 °C, is attributed to the removal of the template (TPABr). The TG curve shows that water and template are completely removed after the temperature of 550 °C. Therefore, this result confirms that the calcination temperature of 550 °C is sufficient for performing the calcinations

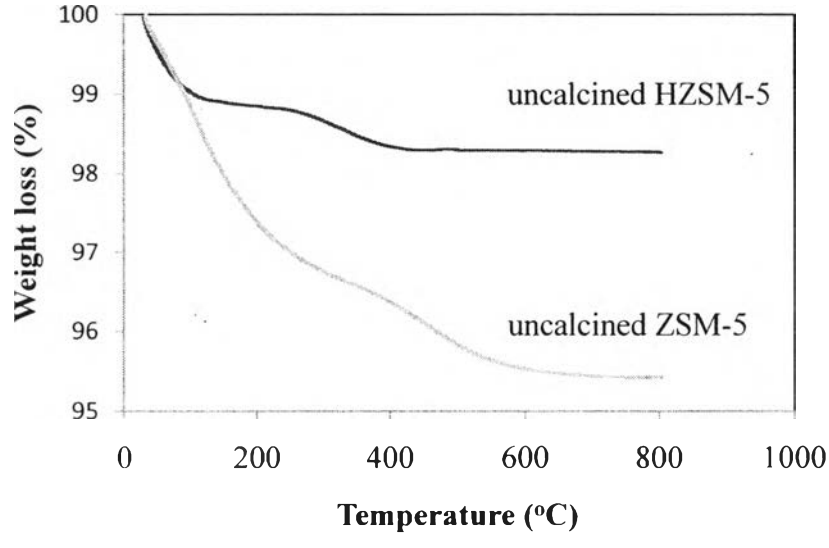

Figure 4.3 TG curves for uncalcined ZSM-5 catalyst and uncalcined HZSM-5 (HZ5A3).

In addition, the TG curve for uncalcined HZSM-5 shows two weight loss regions. The first region, between 100 °C and 200 °C, is caused by the removal of water, whereas the second region, between 300°C and 400°C, is attributed to removal of NH_3. As shown in the figure water and ammonia are completely removed after the temperature of 500 °C. Therefore, this confirms that the calcination temperature of 500 °C is sufficient for performing the calcinations.

4.1.6 TPD of Isopropylamine

The evolution profiles of the m/e = 41 signal obtained from the TPD of adsorbed isopropylamine on HZSM-5 catalysts are shown in Figure 4.4. Isopropylamine decomposes on Brönsted sites by the Hoffman elimination reaction

producing propylene and ammonia (Jongpatiwut *et al.*, 2004). Therefore, quantifying the evolution of propylene as a function of temperature, allows for a reliable determination of the density of strong Brönsted sites taking place at around 306 °C. Accordingly, as shown in Figure 4.4, the density of strong Brönsted acid sites is significantly increased with increasing the synthesized time and synthesized temperature.

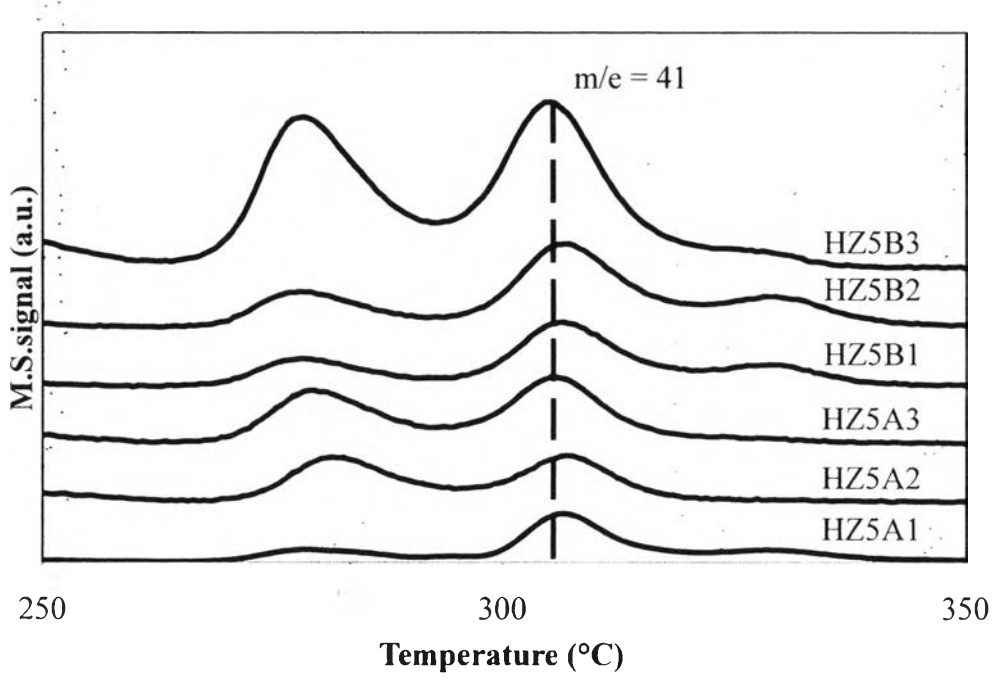

Figure 4.4 Evolution of m/e = 41 during TPD of isopropylamine on HZSM-5 catalysts.

4.2 Catalytic Activity Testing

The catalytic activity of the catalysts was tested in a fixed-bed continuous down-flow reactor. The various parameters including reaction temperature (300 °C to 600 °C), morphology of catalysts, and benzene-to-ethanol ratio (1 to 4) were systematically investigated.

4.2.1 Effect of Temperature

The alkylation of benzene with ethanol was carried out at 300, 500, and 600°C over HZ5B3 at a WHSV of 20 h^{-1} and a B/E ratio of 4. The effect of temperature on the conversions of benzene and ethanol, EB selectivity are shown in Figure 4.5. It shows that the optimum temperature at 500 °C gave the highest benzene and ethanol conversions as well as EB selectivity. As Gao and co-workers (2010) pointed out that the increase in reaction temperature would enhance, the decomposition rate of products, such decomposition led to the increases of benzene and bulkier molecules, which blocked the micropore channels of the catalyst and deactivated the catalyst. On the other hand, at a suitable high temperature, bulkier molecules could diffuse more quickly in the pores, so benzene conversion and EB selectivity at reaction temperature 500 °C were higher than those at 300 °C. However, benzene conversion and EB selectivity at reaction temperature 600 °C were lower than those at 500 °C due to the decomposition of products.

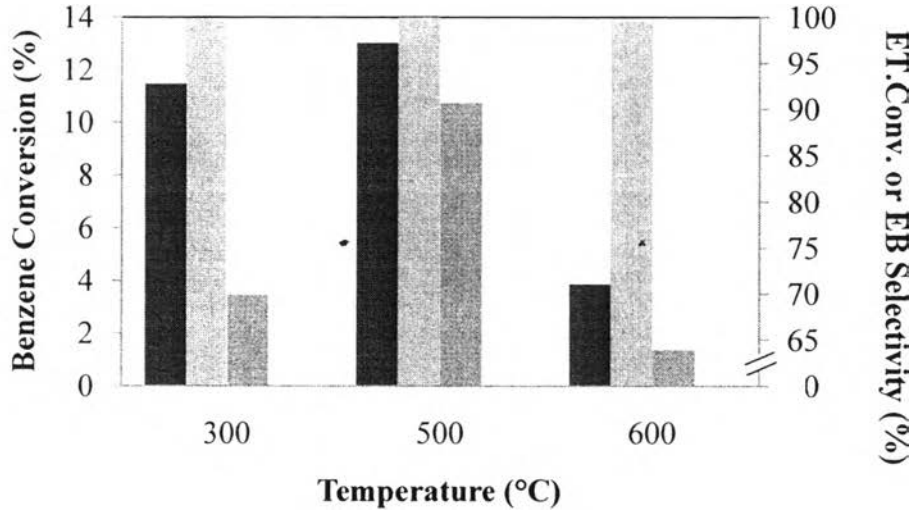

Figure 4.5 Effect of temperature: on (■) benzene conversion, ( ) ethanol conversion, and (▒) EB selectivity for HZ5B3, B/E = 4, and WHSV = 20 h^{-1}.

Table 4.5 Effect of temperature on the products selectivity over HZ5B3[a]

Temperature (°C)	Selectivity (%)					
	Ethylene	EB	Toluene	Xylenes	DEBs	Others[b]
300	0.01	69.85	0.12	0.35	24.98	4.69
500	0.01	90.71	0.23	1.27	6.76	1.03
600	0.05	66.31	8.00	17.83	3.02	4.78

[a] Reaction conditions: B/E = 4, WHSV = 20 h^{-1}, time on stream = 340 minute.

[b] For example, ethyl toluene, propyl benzene, indane, and naphthalene.

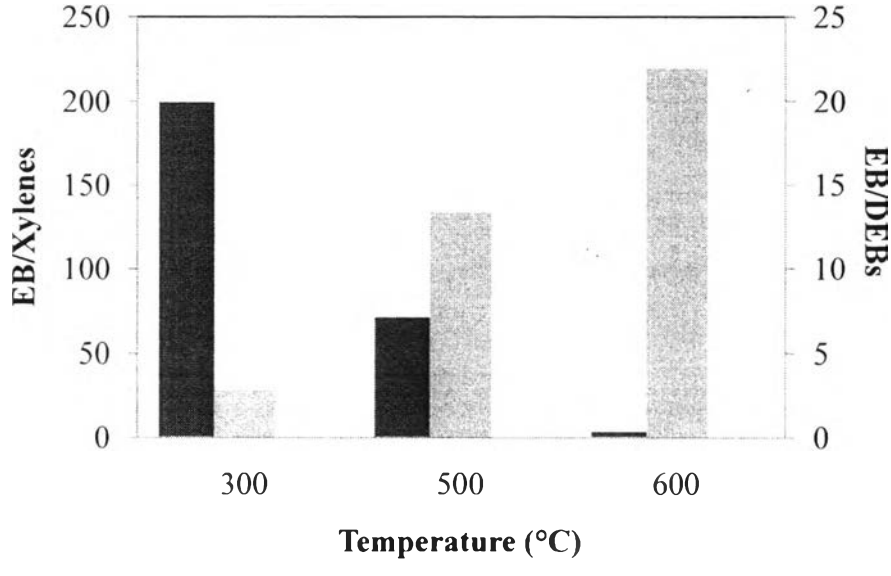

Figure 4.6 Effect of temperature: (■) EB/Xylenes and ( ) EB/DEBs ratios for HZ5B3. B/E = 4, WHSV = 20 h^{-1}, and time on stream = 340 min.

Table 4.5 shows the products selectivity at different temperatures over HZ5B3. It can be observed that reaction carried out at temperature 500 °C provided the highest selectivity to EB (90.71 %). However, the EB selectivity of reaction performed at 300 °C was diminished to 69.85 %, with the DEBs selectivity increased to 24.98 %. When the ratios of EB-to-xylenes and EB-to-DEBs are compared at different temperatures as shown in Figure 4.6, the highest EB-to-DEBs ratio is obtained at 500 °C with a moderate EB-to-Xylenes ratio. This is because the exothermic reaction of the alkylation of EB to DEBs and the endothermic reaction of

the isomerisation of EB to xylenes (Ertl *et al.*, 2008). It should be noticed that at 600 °C, the EB selectivity was declined to 63.93 %, however, the xylenes selectivity was extented to 17.83 %.

4.2.2 Effect of Different Hydrothermal Synthesis Conditions

Figure 4.8 shows the catalytic activity of the synthesized HZSM-5 catalysts. The HZ5A2 catalyst provided the highest benzene conversion and EB selectivity. As seen in Table 4.2, the M/T ratio for HZ5A2 was almost lowest indicating the dominance of mesopore volume. From the shape selectivity point of view, it would allow EB to diffuse out of the pores easier than the others having the plentiful of micropore volume. Therefore, it is postulated that a higher total pore volume and lower micropore volume of the catalysts would give a higher yield of EB.

Moreover, this revealed that the crystal size can affect the ethylbenzene selectivity. If the crystal was too large, ethylbenzene did not diffuse from the pore quickly, so the secondary reactions increased. This observation is in good agreement with that of Gao et al. (2010).

In addition, it is well known that acidity plays an important role in alkylation reactions and it can affect the products selectivity. The HZ5A2 provided the highest EB selectivity as the Brönsted acid sites of HZ5A2 were observed to be the lowest. This is also in agreement with Li et al. (2009). Therefore, the other effects on the catalyst performance were studied on the HZ5A2 catalyst.

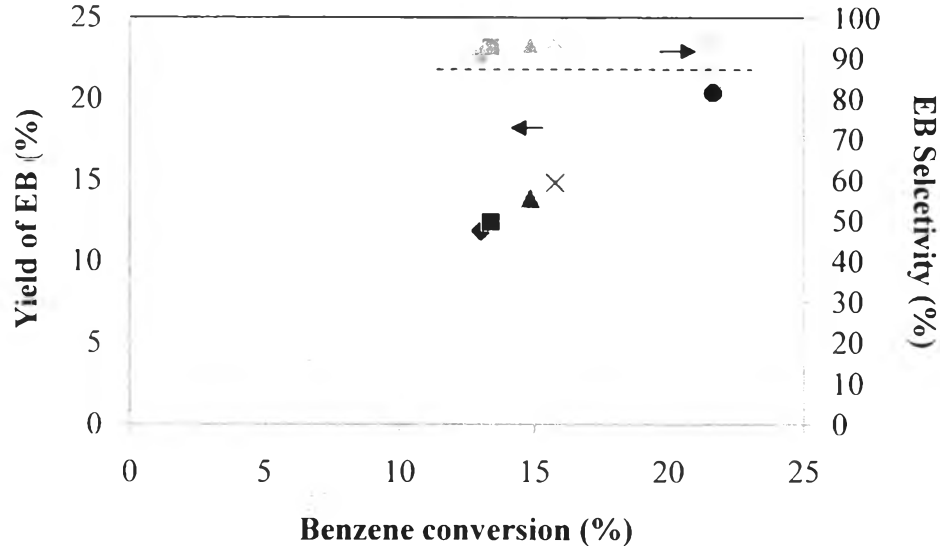

Figure 4.8 Catalytic activity of the synthesized HZSM-5 catalysts : HZ5A2 (●), HZ5A3 (X), HZ5B1 (▲), HZ5B2 (■), and HZ5B3 (♦), at B/E = 4, WHSV = 20 h^{-1}, temperature 500 °C, and TOS = 340 min.

4.2.3 Effect of B/E Feed Ratio

The effect of B/E feed ratio was studied by varying the benzene to ethanol (B/E) feed molar ratios from 1 to 4 over the HZ5A2 at 500 °C and a WHSV 20 h^{-1}. The benzene and ethanol conversions as a function of B/E ratio are shown in Figure 4.9. It shows that the benzene and ethanol conversions were significantly declined as a B/E feed ratio was increased from 1 to 4. This is probably because the dilution of ethanol by benzene. The probability of benzene interacting with ethyl cations is reduced, and then the reduction of benzene and ethanol conversion is obtained (Odedairo *et al.*, 2010).

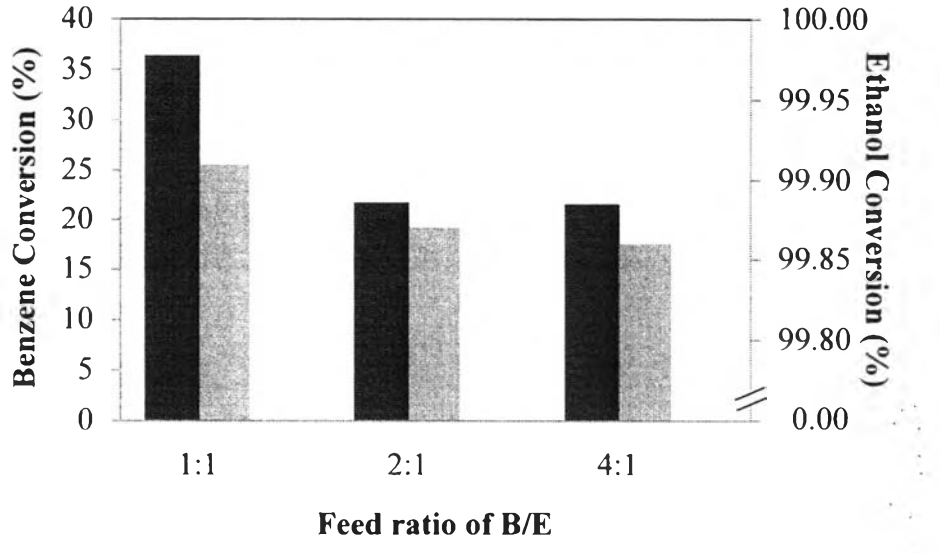

Figure 4.9 Effect of B/E feed ratio: on (■) benzene conversion and ( ) ethanol conversion for HZ5A2, WHSV = 20 h^{-1}, temperature = 500 °C, and TOS 340 min.

Table 4.6 Effect of B/E feed ratio on the products selectivity over HZ5A2[a]

B/E feed ratio	Selectivity (%)					
	Ethylene	EB	Toluene	Xylenes	DEBs	Others[b]
1:1	0.01	90.37	0.1	0.45	8.56	0.51
2:1	0.01	92.50	0.17	0.74	5.91	0.67
4:1	0.02	94.13	0.2	0.88	3.84	0.92

[a] Reaction conditions: T = 500 °C, WHSV = 20 h^{-1}, time on stream = 6 h.

[b] For example, ethyl toluene, propyl benzene, indane, and naphthalene.

Table 4.6 presents the effect of B/E feed ratio on the products selectivity. The selectivity to EB was increased with increasing B/E feed ratio whereas the selectivity to DEB isomers was decreased. This might be also resulted from the dilution of ethanol. The high EB selectivity at higher benzene to ethanol ratios was attributed to the suppression of further alkylation of EB by ethyl cations. (Odedairo *et al.*, 2010).

4.2.4 Coke Formation

The spent catalysts were analyzed by the temperature programmed oxidation (TPO) technique to observe the coke formation over the synthesized HZ5A2 catalyst under different B/E feed ratios at reaction conditions: T = 500°C, WHSV 20 h^{-1}, and time on stream 340 min. The results are presented in Table 4.7.

Table 4.7 Coke formation of the spent HZ5A2 catalyst

B/E feed ratio	Coke formation (wt%)
1:1	0.086
2:1	0.109
4:1	0.295

As shown in Table 4.7, the amount of coke deposit over the spent HZ5A2 at B/E ratio of 1, 2, and 4 is 0.086, 0.109, and 0.295 wt%, respectively. With increasing the amount of benzene in feed, the coke formation would increase because the benzene could be cracked easier at higher amount resulting in enhancing the tendency of coke formation.